Available online at www.sciencedirect.com

ScienceDirect

Procedia CIRP 74 (2018) 475–480

www.elsevier.com/locate/procedia

10th CIRP Conference on Photonic Technologies [LANE 2018]

Description of the influence of two laser intensities on the spatter formation on laser welding of steel

Falk Nagel[a,]*, Lucas Brömme[a], Jean Pierre Bergmann[a]

[a]*Technische Universität Ilmenau, Department of mechanical engineering, Production Technology Group, Gustav-Kirchhoff-Platz 2, Ilmenau 98693, Germany*

* Corresponding author. Tel.: +49 367769 2980 ; fax: +49 367769 1680. *E-mail:* info.fertigungstechnik@tu-ilmenau.de

Abstract

The reduction of spatter formation for deep penetration laser welding with the application of welding speeds over 8 m/min is the subject of the presented proceeding. Thereby, two laser spots are spatially superposed. Due to the application of the second laser spot an enlargement of the capillary was detected. Furthermore, a significant reduction of the loss of mass due to spatter was achieved. Moreover, the influence of the lateral displacement of the second spot relative to the first laser was analyzed.

Peer-review under responsibility of the Bayerisches Laserzentrum GmbH.

Keywords: Laser, welding, spattering, capillary, steel

1. Introduction

The continuous development in the field of solid state lasers leads to a steady enhancement of applicable laser powers. Simultaneously, the quality of the laser beam remains at a constant level or has been improved, respectively. Thus, higher intensities are appropriately result in higher travel speed. The development can be traced back to the demands for laser cutting. In contrast to the laser cutting process, the increase of the travel speed leads to spatter formation for laser beam welding. The spatter formation occurs for all welding speeds. But at a certain welding speed, the spatter formation changes from a chaotic to an orientated behavior. Here a distinct increase of loss of material in the weld seam can be observed for the orientated spatter behavior. This loss can lead to underfill and decrease of mechanical properties of the weld seam. For this reason, the reduction of spatter is of high commercial interest such as for pipe welding or welding of tailored blanks.

2. State of the Art

The spatter formation helps account for the stability of the welding process, because the formation is linked to the process dynamics. A droplet escapes the melt pool if the energy of the fluid element (E_{kinFl}) within the melt pool exceeds the energy of the escaping fluid element (E_{kinDr}) and the surface energy of melt E_{SurDr} (see Eq. 1 and Eq 2) [1]:

$$E_{kinFl} > E_{kinDr} + E_{SurDr}\,. \tag{1}$$

Here, ρ represents the density of the metal, V the volume of the fluid element, v the velocity, σ the surface tension and O the surface of the droplet:

$$\frac{\rho V_{Dr}\left|\vec{v}_{Fl}\right|^2}{2} \geq \frac{\rho V_{Dr}\left|\vec{v}_{Dr}\right|^2}{2} + \sigma O_{Dr}\,. \tag{2}$$

The formation of spatter can be explained by two reasons. The first explanation is based on the instable capillary wall. Here the interaction between metal vapor and melt at the front and rear wall of the capillary result in a formation of small droplets [2]. This appearance is typical for low welding speeds. The second explanation relates to the flow condition within the melt pool [2-4]. Here the metal vapor which emerges at the front of the capillary transfers its momentum to

2212-8271
Peer-review under responsibility of the Bayerisches Laserzentrum GmbH.
10.1016/j.procir.2018.08.147

the fluid element at the back side of the capillary. Because of this flow, the local volume at the backside of the capillary exhibits a vertical flow component [6]. Thus, a wave at the back side of the capillary is formed, and if the energy of the fluid element exceeds a certain value, the element escapes the melt pool. This appearance is occurs at higher welding speeds.

In order to reduce the spatter formation, several approaches have been investigated. Less spatter was determined for laser wavelength of 10 µm compared to a wavelength of 1 µm. It is assumed that the plasma absorption of the laser beam leads to higher temperature within the capillary, resulting in a stabilized capillary [7]. The influence of a shielding gas flow was reviewed and a stabilizing effect on the capillary was detected. Consequently, a reduction of the spatter formation was achieved [8]. Furthermore, the ambient pressure was reduced and a reduction of the spatter was determined qualitatively [9]. Another approach is the use of a scanning systems realizing a spatial oscillating [10, 11].

The use of non-standard intensity distributions for reducing the spatter formation is the subject of several research teams. It was shown that the use of twin spots can have a positive influence [12]. The use of a coaxial fiber optic cable results in the formation of ring and circular intensity distribution on the workpiece. It is reported that the loss of mass can be reduced significantly with minor occurrence of spatter [13]. Further, due to the spatial superposition of two laser spots, an increase of the weld bead at the top surface can be achieved. It can be assumed that the increased weld bead leads to a reduction of the fluid flow within the melt pool. Further, an impact of the additional heat input on the capillary might lead to further evaporation. The preceding investigations have been conducted for full penetration welding. Plus, the positive influence of the second, super positioned spot on the spatter formation was demonstrated [14, 15].

This proceeding shows the influence of the lateral shift of the second spot on the aperture of the capillary and the resulting spatter formation. Furthermore, the influence of two spot sizes on the resulting spatter formation will be given for partial deep laser welding.

3. Experimental Procedure

Table 1. Chemical composition of 1.4301 (AISI 304) according to the Datasheet [16]

Cr	Ni	C	Si	Mn	Fe
17-19	8-10	≤ 0,07	≤ 1	≤ 2	Bal.

The stainless austenitic steel 1.4301 (X5CrNi18 10, Type 304) was used for the experimental trails. The chemical composition is summarized in Table 1. The dimensions of the sheets as well as the position of the weld seam can be found in Fig. 1.

The specimens were placed in a sample carrier and the pneumatic positioner (hold down force of 295 N) fixed the plate. The sample carrier was moved with an industrial robot (KR 60HA, KUKA AG). The experiments were carried out using a TruDisk 5000.75 (Trumpf Laser- und Systemtechnik GmbH) disc laser and a diode laser (LDM 3000, Laserline GmbH). The setup and properties of the two lasers are summarized in Table 2.

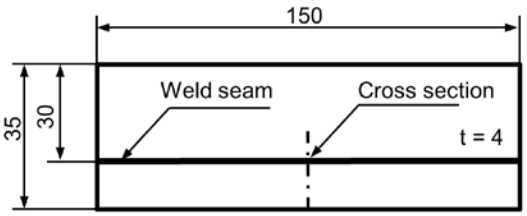

Fig. 1. Dimensions of the specimen in [mm]

Table 2. Settings of the laser sources

Manufacture	TruDisk 5000.75 Trumpf	LDM 3000 Laserline
Wavelength	1030 nm	980 nm
Fiber diameter	200 µm	1000 µm
Focal length collimation	200 mm	70 mm, 100mm
Focal length focus	280 mm	100 mm, 200mm
Spot diameter	274 µm	1.4 mm x 2.0 mm 2.0mm x 2.8mm
Laser power	var.	var.
Angle of incidence	90°	45°
Focal position	0 mm	0 mm
M²	23.5	274.9; 266.9
Rayleigh length	2.38 mm	5.11 mm; 9.028 mm

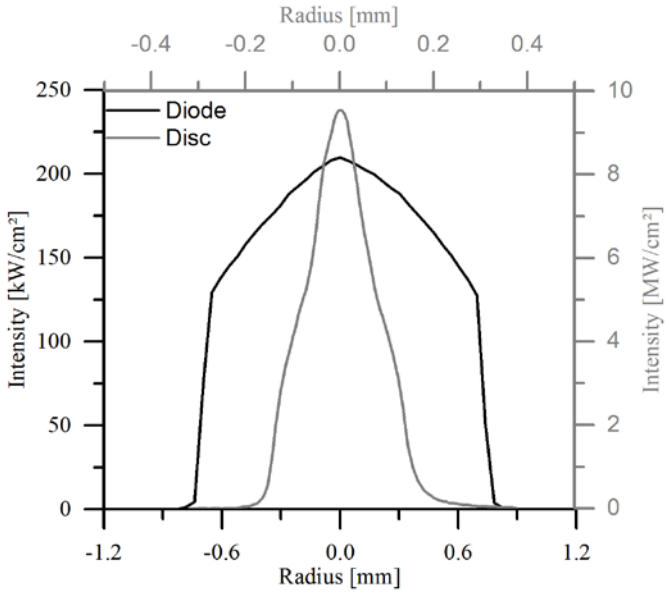

Fig. 2. Intensity distribution of the disc and diode laser

The intensity distribution of the two laser sources was measured using a FocusMonitor, Primes GmbH. The intensity distributions in focal plane are summarized in Fig. 2. Here, a laser power of 3000 W was used for the disc laser and 2500 W for the diode laser.

Due to the angle of incidence for the diode laser (see Fig. 3), an elliptical spot is depicted on the workpiece. The spot position of the diode laser in relation to the disc laser spot was set 0.5 mm in front and behind the disc laser spot.

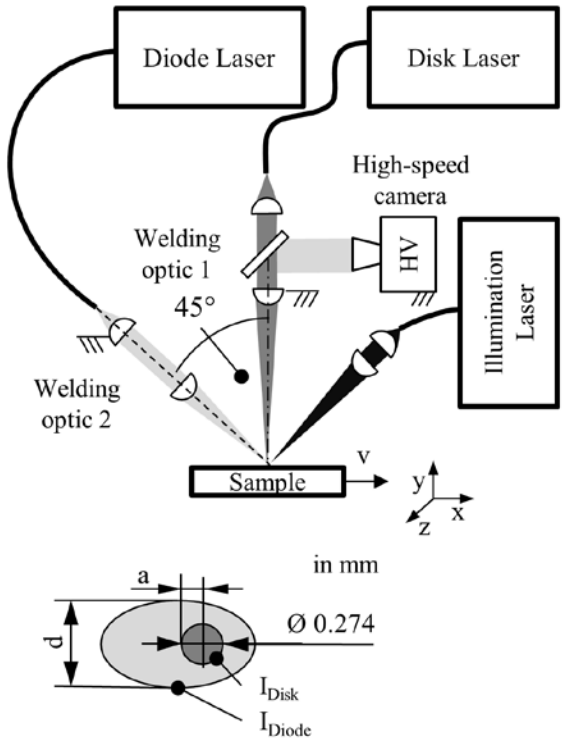

Fig. 3. Schematic illustration of the experimental setup

The laser power of the disc laser was set realizing a bead on the plate with a depth of 2 mm. The observation of the capillary was achieved due to the use of a vis-coated mirror within the beam path of the laser light (see Fig. 3) and the Photron high speed camera SA-X2. The Navitar 12x objective without the focusing lens was used. The weld pool was illuminated under the application of the Cavilux laser, Cavitar Ltd. A narrow bandpass filter for the wavelength of 808 nm was placed in front of the camera sensor. The footage was analyzed manually by detecting the edges of the capillary in each picture. Here, the capillary appears brighter than the surrounding weld pool.

For quantifying the loss of material, the high precision balance (Kern PLJ 2000-3A) was used. The readout amounts to 0.001 g, and the reproducibility is given with ± 0.002 g. The mass of the sample was determined before and after the welding process calculating the loss of mass. The experiments were performed three times receiving a statistical prediction.

4. Results

First, the loss of mass is characterized for the reference process and applying the superposition of the second laser spot. The results are shown Fig. 4. Concerning the reference process, the loss of mass amounts to 0.03 mg/mm for a welding speed of 8 m/min. No spatter was observed and the loss of mass can be ascribed to evaporation. The loss of mass rises to 1.16 mg/mm for a welding speed of 12 m/min. Due to the further increase of the welding speed, the loss of mass decreases to 0.74 mg/mm for a welding speed of 20 m/min. This characteristic curve is similar to the results using austenitic stainless steel 1.4571 for full penetration welding [14].As opposed to this, the loss of mass amount less than 0.3 mg/mm for the welding speed ranges from 8 mm/min to 20 m/min using the super positioned second laser spot. Further, the loss of mass reduces with the increase of the laser power from 1 kW to 1.5 kW. The application of the larger spot size of the diode laser under the assumption of a similar intensity leads to a reduction of the loss of mass as well. But in comparison to the smaller spot size, the loss of mass is 0.1 mg/mm higher for the welding speed range from 8 m/min to 16 m/min. Examining the results for a welding speed of 20 m/min, a higher loss of mass was determined for the smaller spot size than for the larger.

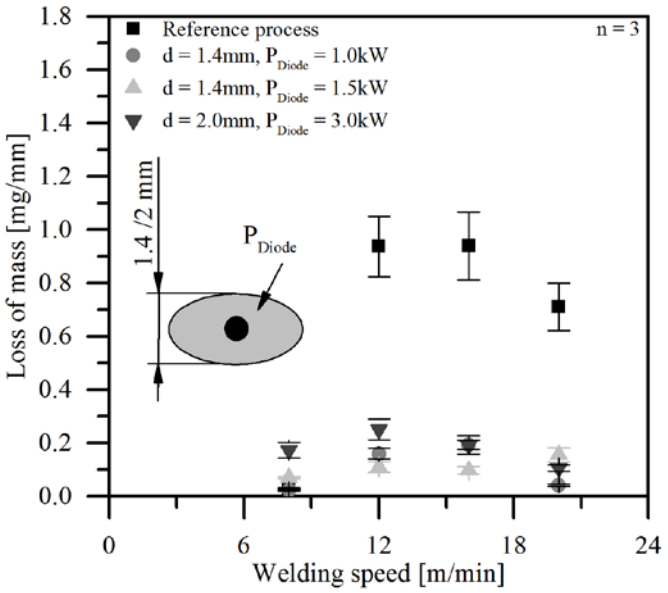

Fig. 4. Influence of the second laser spot on the loss of mass

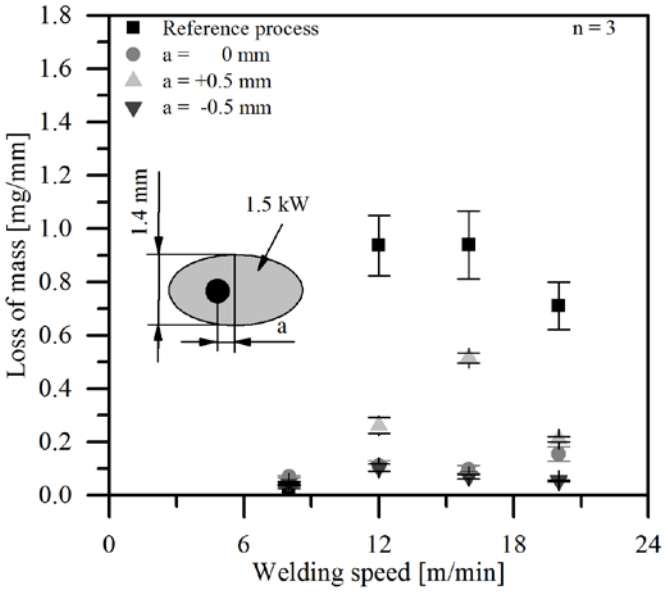

Fig. 5. Influence of the relative position between the two laser spots

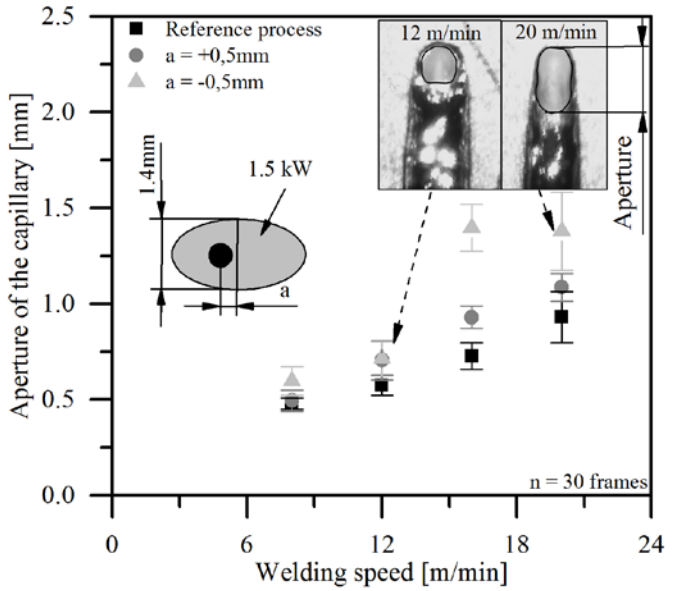

Fig. 6. Influence of the superposition on the aperture of the capillary

Table 3. Parameters of the linear regression

	linear regression	Coefficient of determination R^2
Reference process	y =0.15 + 0.037*x	0.799
Superposition, a = 0.5mm	y = 0.10+ 0.049*x	0.89
Superposition, a = -0.5mm	y = -0.035 + 0.075*x	0.74

The influence of the relative displacement between the two laser intensities is given in Fig. 5. Here a rise of loss of mass was identified for the precursory positioned diode laser spot. The outcome is distinct for the welding speed of 16 m/min. The use of a non-displacement and trailing position of the diode laser spot leads to a higher reduction in the loss of mass.

The observation of the capillary reveals a manipulation of the aperture of the capillary due to the welding speed and the application of the diode laser. The influence of the welding speed on the aperture of the capillary is summarized in Fig. 6. The aperture of the capillary rises with increasing welding speed, and a linear correlation can be determined according to Table 3. The application of the second spot leads to an enlarged aperture of the capillary, which can be observed in Fig. 6. On this occasion, the linear regression (Table 3) reveals a higher slope using the trailing laser spot than with the precursory positioned laser spot. It should be mentioned that the aperture of the capillary applying a welding speed of 16 m/min and a trailing position laser spot exhibits a higher value in comparison to the other parameters. Hence, a low coefficient of determination is the result of the linear regression. This outcome cannot be explained so far and will be the subject of a further investigation.

Fig. 7 and Fig. 8 show the resulting weld bead formation in the metallographic cross sections. Considering the reference process, the weld seam is narrowly developed. A good weld reinforcement can be observed for a welding speed of 8 m/min. For the increased welding speed, a slight formation of undercut can be identified. The width of the weld seam decreases with increasing welding speed (see Fig. 9). However, the penetration depth keeps constant for the increasing welding speed (see Fig. 10).

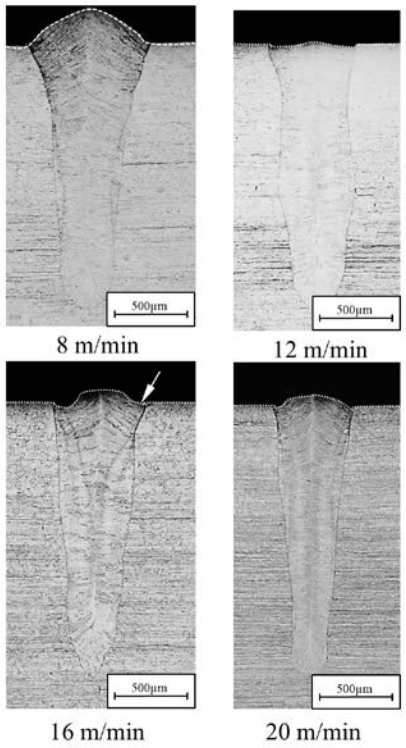

Fig. 7. Cross section of the reference process

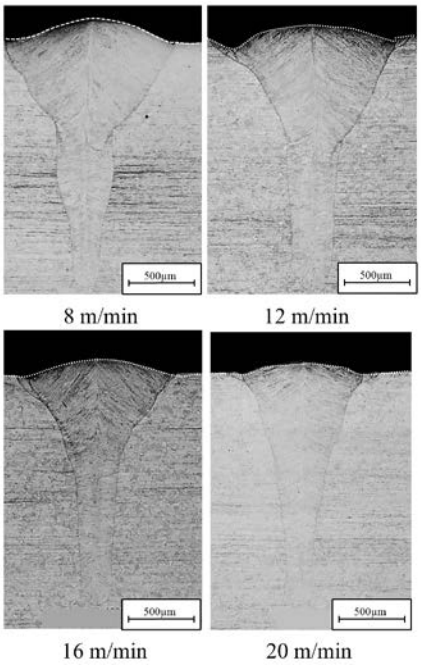

Fig. 8. Cross section using the superposition

Observing the metallographic cross sections using the second laser spot, a y-shaped weld bead formation can be identified. Here the y-shape turns into a v-shape with increasing welding speed (see Fig. 8). Additionally, the width of the weld seam decreases with increasing welding speed (see Fig. 9). The depth of the weld bead which is caused by the diode laser decreases with increasing welding speed.

Considering the penetration depth (see Fig. 10), a slight increase of the penetration depth was detected for the welding speed of 8 m/min and the diode laser power of 1.5 kW. But this value is attributed to outliers.

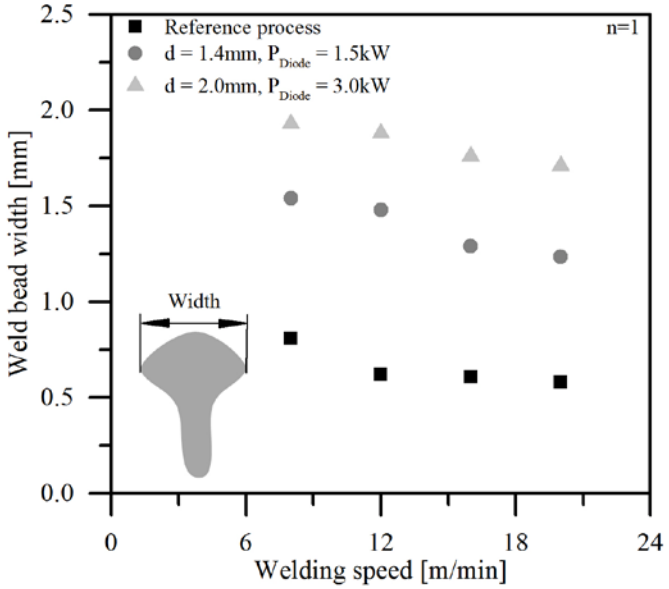

Fig. 9. Influence of the superposition on the width of the weld seam

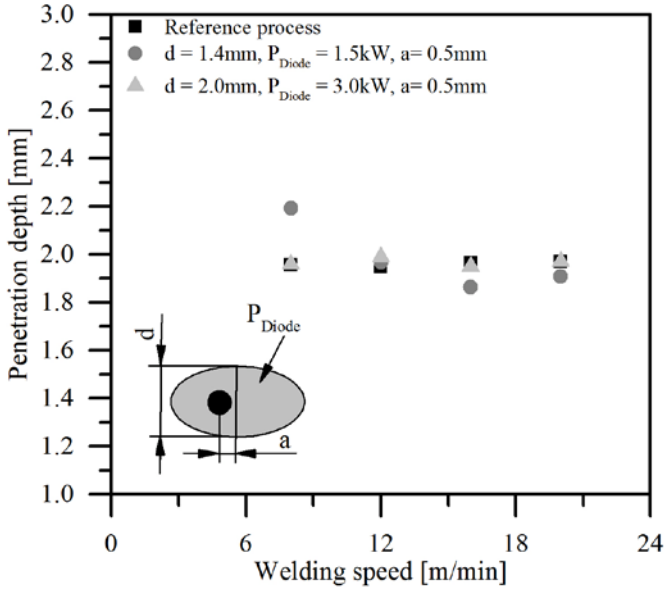

Fig. 10. Influence of the superposition on the penetration depth

5. Discussion

The inspection of the cross sections will serve as the starting point of the discussion. The inspection reveals a constant penetration depth for the reference process, which can be explained due to the application of a constant energy per unit length. The application of the second laser spot leads to a slight increase of the penetration depth for 8 m/min. This appearance can be explained by the additional heat input. But it can be assumed that this value is an exception. The inspection exposes a distinct increase of the weld bead at the upper side due to the application of the second laser spot. The decrease of the depth of the additional weld bead can be explained by the fact that a constant laser power was used. Thus, the increase of the welding speed and the constant thermal conductivity of the material lead to a decrease of the width and depth of diode laser based weld bead formation.

Concerning the aperture of the capillary, a linear relation between the welding speed and the aperture was determined. This appearance is known in the literature [17]. The absorbed intensity rises with higher welding speeds, resulting in a higher ablation rate. Hence, the vapor impinges on the back side of the capillary with an increased velocity. Consequently, the dynamic pressure of the metal vapor increases, which leads to the enlargement of the aperture of the capillary.

Due to the use of the super positioned second spot, the aperture of the capillary increases with a higher slope compared to the reference process. It can be assumed that the intensity of the second laser spot leads to an additional evaporation at the back side of the capillary. It should be noted that the temperature of the melt at the back side of the capillary is close to the evaporation temperature, and the additional energy input would lead to the supplemental evaporation. This appearance allows an enlargement of the capillary. The influence of the position of the second laser spot can only be explained by the intensity distribution of the diode laser which is not a distinct top hat distribution. The intensity at the edge is about 25 % lower than at the center of the spot. Due to the longitudinal shift of the second laser spot towards the back side of the capillary, the peak of the intensity distribution of the diode laser is focused on the back side of the capillary. This can lead to an increased evaporation.

Another explanation of the increased aperture of the capillary can be given by the aspect of the increased weld bead size. It can be assumed that the increased weld bead results in an influence of the flow conditions within the melt pool due to the increased flown through area. An impact of the shift between the two laser spots on the increased aperture of the capillary cannot be given for this explanation. Besides, the upper area of the weld bead decreases with increasing welding speed using a constant diode laser power. Thus, the ability to reduce the flow lowers with increasing welding speed. It can be concluded that the influence of the increased weld bead area is not significant.

In terms of the loss of mass, an influence of the welding speed on the loss of mass was identified. Here no linear correlation between welding speed and the loss of mass can be accounted for. Furthermore, no relation between the aperture of the capillary and the loss of mass can be identified. But it can be assumed that the interaction between the degassing metal vapor and the melt at the back side of the capillary is reduced. Hence, the droplet escape condition is not fulfilled and fewer droplets escape the melt pool. The observation of the interaction of the metal vapor and the melt will be the subject of further examinations

6. Conclusions

This proceeding shows the reducing effect of the superposition of two laser spots on the spatter formation. The application of the second spot leads to an increase of the

upper weld bead size. Further, an increase of the aperture of the capillary was recognized. Here, an influence of the longitudinal position between the two laser spots was identified. It is supposed that the intensity of the second spot results in an additional evaporation and, due to the intensity distribution of the diode laser, the influence of the position is explainable. Further, an influence of the relative position between the two spots on the loss of mass was determined. Likewise, the trailing position leads to further reduction of the loss of mass. Nevertheless, an impact of the second laser spot on the weld pool dynamics has to be taken into account. Assumptions of the operating principles are given and discussed briefly.

For further investigation, the inspection of the weld pool dynamics using x-ray particle tracing and numerical simulation methods are planned. The influence of the orientation of the diode laser (pull and push technique) will be presented in a further publication. Moreover, the influence of the metal vapor on the spatter behavior will be investigated.

Acknowledgements

The IGF-Investigation 18582 BR of the investigation federation “Forschungsvereinigung Schweißen und verwandte Verfahren e.V. des DVS”, Aachener Straße 182, 40223 Düsseldorf, Germany was founded resulting from the program “Förderung der industriellen Gemeinschaftsforschung” (IGF) by the Federal Ministry of Economic Affairs and Energy based on a resolution of the German Parliament. We would like to thank all funding organizations.

References

[1] Hügel, H, Graf, T. Laser in der Fertigung. 3rd ed. (german), Springer Vieweg, Wiesbaden; 2014.

[2] Zhang M J, Chen G Y, Zhou Y, Li SC; Deng H. Observation of spatter formation mechanisms in high-power fiber laser welding of thickplate In: Applied Surface Science 280, p.868-875. 2013.

[3] Volpp J. Keyhole stability during laser welding—Part II, Process pores and spatters. In: Production Engineering, no. 11, p. 9–18. 2017.

[4] Fabbro R, Slimani S, Doudet I, Coste F, Briand F. Experimental study of the dynamical coupling between the induced vapour plume and the melt pool for Nd–Yag CW laser weldinging In: Journal of Physics D: Applied Physics, vol. 39, no. 2, p. 394–400. 2010.

[5] Kaplan A F H, Powell J. Spatter in Laser welding, In: Journal of laser Applications vol. 23. no. 3. 2011.

[6] Katayama S, Tsukamotot S, Fabbro R, (Ed. Katayama, S.): Handbook of laser welding technologies. Cambridge: Woodhead Publishing. 2013.

[7] Rominger V, Schäfer P, Weber R, Graf Th In: Prozessuntersuchungen beim Laserstrahltiefschweißen – Festkörperlaser hoher Brillanz im Vergleich zu CO_2-Laser, DVS –Bericht,p. 188-193. 2010.

[8] Kamimuki K, Inoue T, Yasuda K. et al. Prevention of welding defect by side gas flow and its monitoring method in continuous wave Nd:YAG laser welding. In: Journal of Laser Applications, vol.14, no. 3. p. 136-145 2002.

[9] Rominger V, Harrer T, Keßler S, Braun H, Dorsch F, Abt F, Jarwitz M, Heider A, Weber R, Graf T: Formation mechanism of process instabilities and strategies to improve welding quality. In: conference proceeding, ICALEO, 2012.

[10] Schweier M, Heins JF, Haubold MW, Zäh MF. Spatter formation in laser welding with beam oscillation. In: LIM Conference 2013, Physics Procedia, no.41, p 20-30. 2013.

[11] Standfuß J, Beyer E. Innovations in laser welding using high brightness lasers. In: International Lasersymposium Fiber and Disc (FiSC 2012), Stuttgart: Fraunhofer Verlag. 2012.

[12] Trautmann A. Bifocal Hybrid Laser Welding – A Technology for Welding of Aluminium and Zinc-Coated Steels. PhD-Thesis TU München. München. 2008.

[13] Speker N, Haug P., S. Feuchtenbeiner, T. Hesse, D. Havrilla: BrightLine weld-spatter reduced high speed welding with disk lasers, conference paper, SPIE LASE, San Francisco, 2018.

[14] Nagel, F., Stambke, M., Bergmann, J.P.: Reduction of spatter formation by superposition of two laser intensities, conference paper, ICALEO, San Diego, 2016.

[15] Nagel, F., Drechsel, C., Bergmann, J.P.: Reduction of the spatter formation due to the use of superposition of two laser intensities, conference paper, Laser in Manufacturing, München, 2017.

[16] Datasheet of 1.4301 https://www.dew-stahl.com/fileadmin/files/dew-stahl.com/documents/Publikationen/Werkstoffdatenblaetter/RSH/1.4301_de.pdf

[17] Weberpals, J.P., Dausinger, F.: Fundamental understanding of spatter behavior at laser welding of steel, P# 704, ICALEO, 2008.